

Electronic supplementary information (ESI) available

# **Carbon Quantum Dots Embedded with Mesoporous Hematite Nanospheres as Efficient Visible Light-active Photocatalysts**

*Byong Yong Yu and Seung-Yeop Kwak\**

Department of Materials Science and Engineering, Seoul National University,  
599 Gwanak-ro, Gwanak-gu, Seoul, Korea

\* To whom correspondence should be addressed. *E-mail:* sykwak@snu.ac.kr.

*Tel:* +82-2-880-8365, *Fax:* +82-2-885-1748

**Table S1.** FWHM values of the main diffraction peaks and the crystallite size for mesoporous hematite with the respective diffraction planes.

h k l	$2\theta$ (deg.)	$d$ -spacing (nm)	Intensity (a.u.)	FWHM ( $2\theta$ )	Crystallite size (nm)
0 1 2	24.10	0.36	28.1	0.34	23.63
1 0 4	33.10	0.27	100.0	0.36	22.77
1 1 0	35.56	0.25	70.7	0.36	22.92
1 1 3	40.80	0.22	23.2	0.36	23.29
0 2 4	49.42	0.18	34.1	0.38	22.76
1 1 6	54.02	0.17	45.1	0.38	23.21
2 1 4	62.40	0.15	28.4	0.38	24.17
3 0 0	63.98	0.14	25.4	0.38	24.38

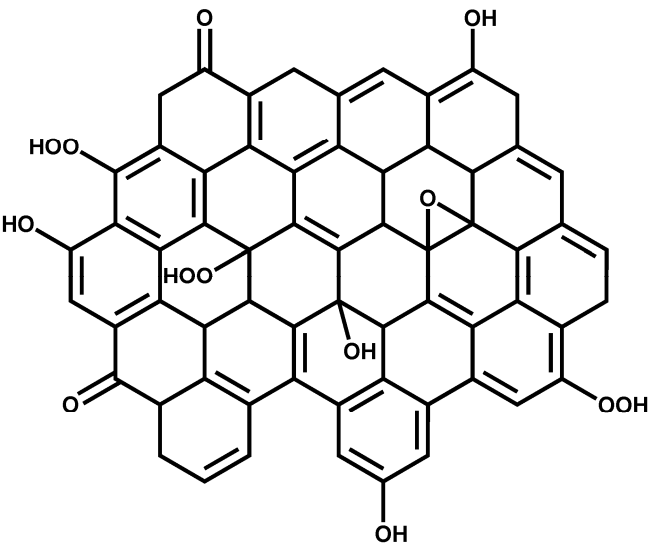


**Fig. S1** Chemical structure of CQD.

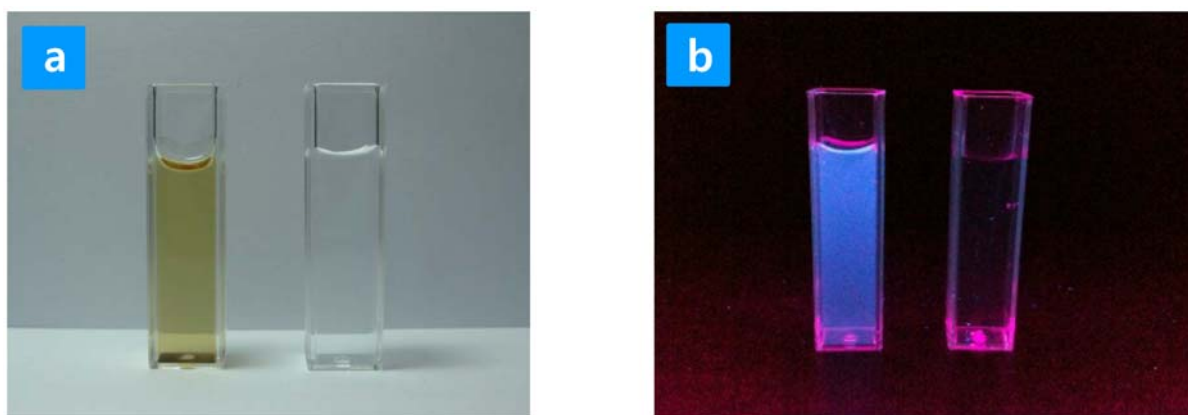


**Fig. S2** CQDs optical image in water illuminated under (a) white (left; CQDs in water, right; water) and (b) UV light (left; CQDs in water, right; water).

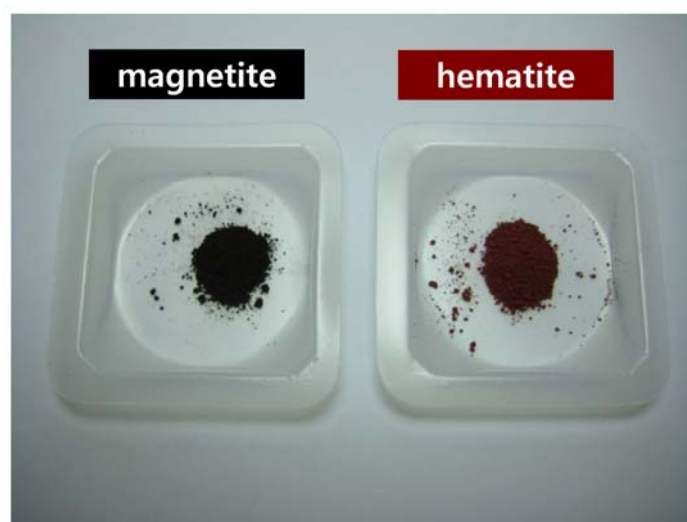


**Fig. S3** Photograph of mesoporous magnetite and hematite powders.

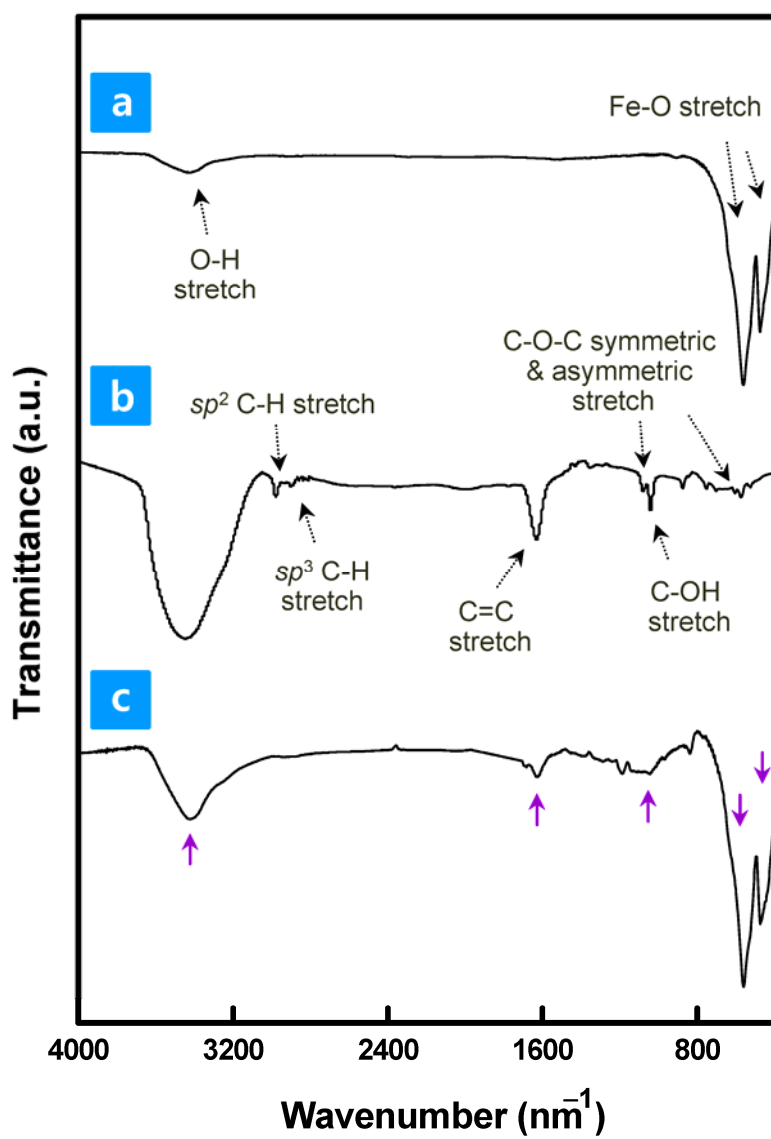


**Fig. S4** FT-IR spectrum of (a) MH, (b) CQD, and (c) CQD/MH.

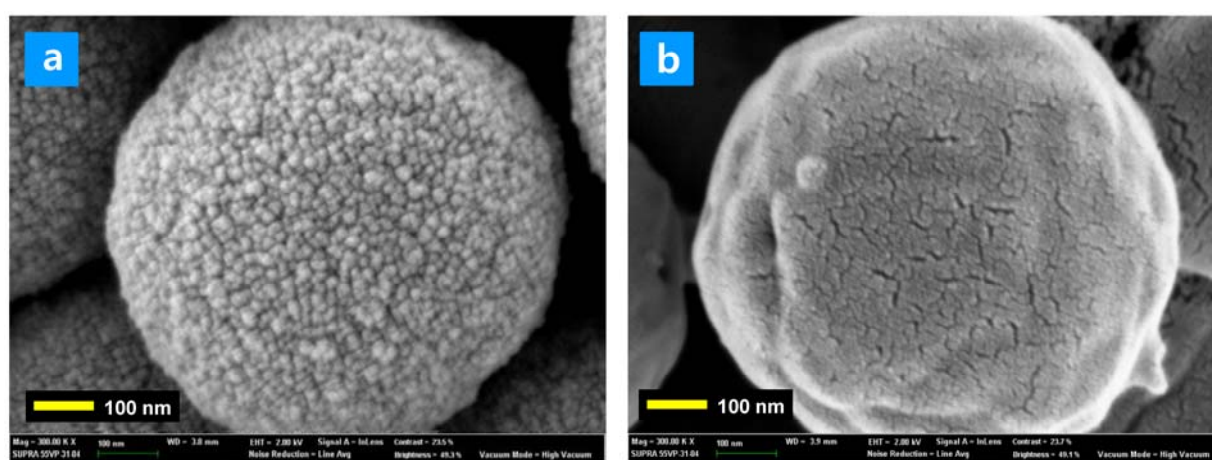


**Fig. S5** FE-SEM images of (a) MH, and (b) CQD/MH (a more detailed view).

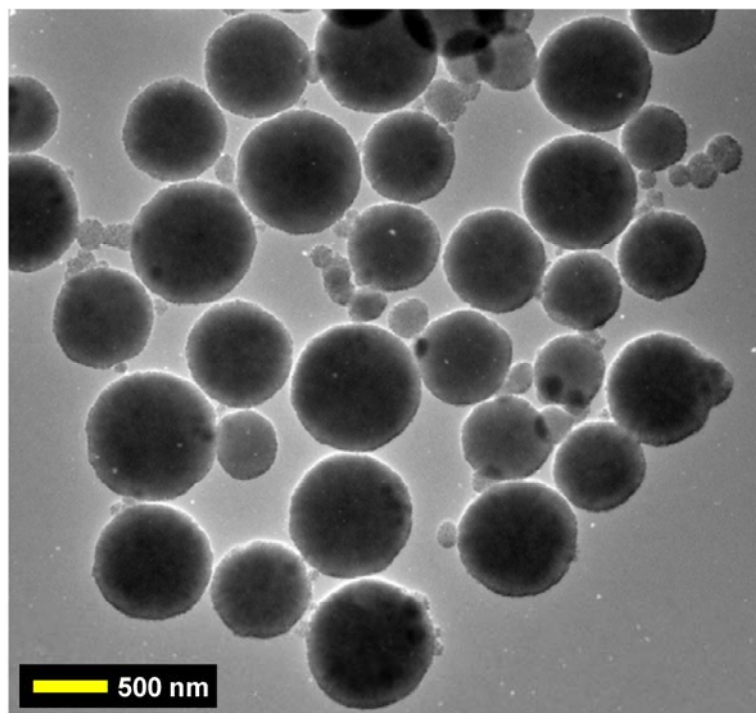


**Fig. S6** TEM images of CQD/MH hybrid clusters.



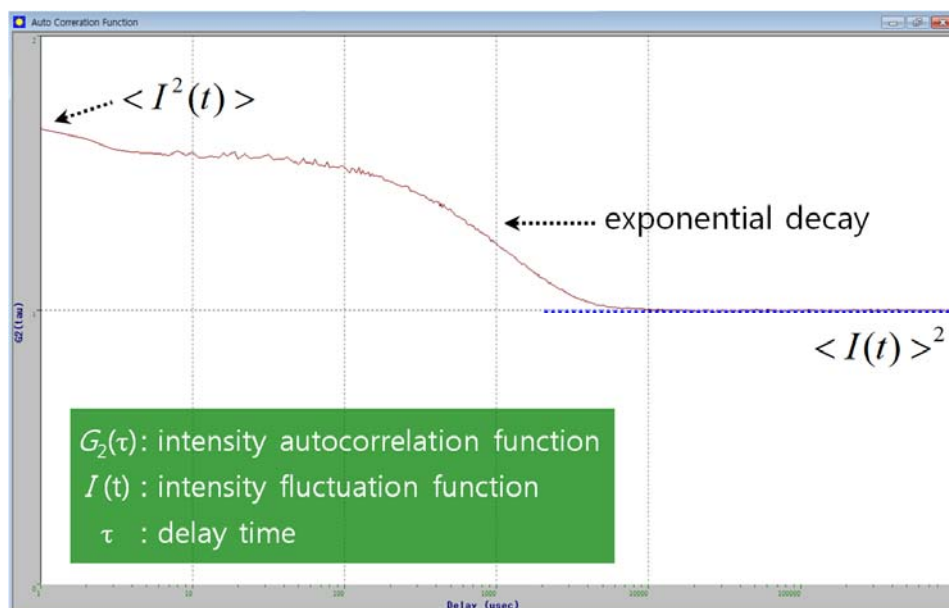
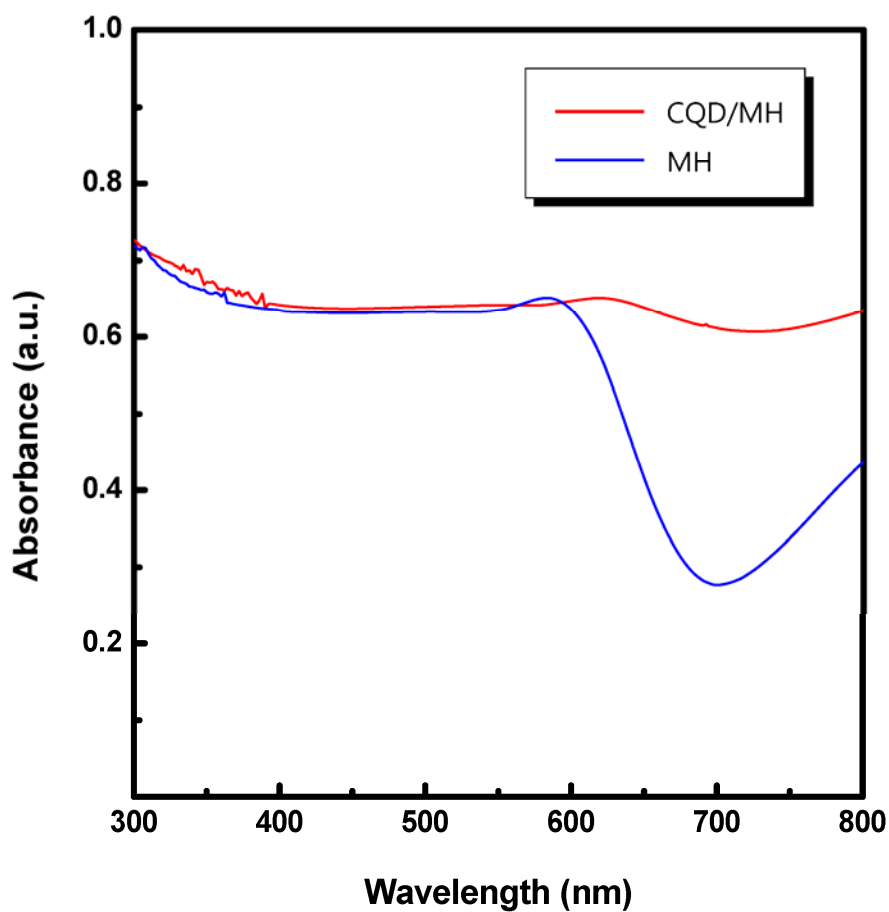


**Fig. S7** The intensity auto-correlation function (ACF),  $G_2(\tau)$  for CQD/MH sample in DLS.

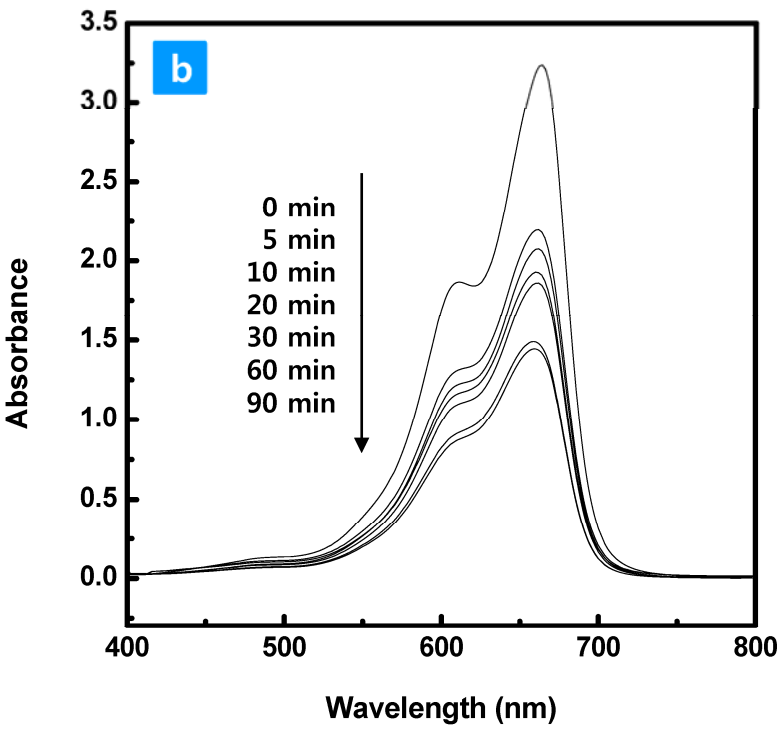
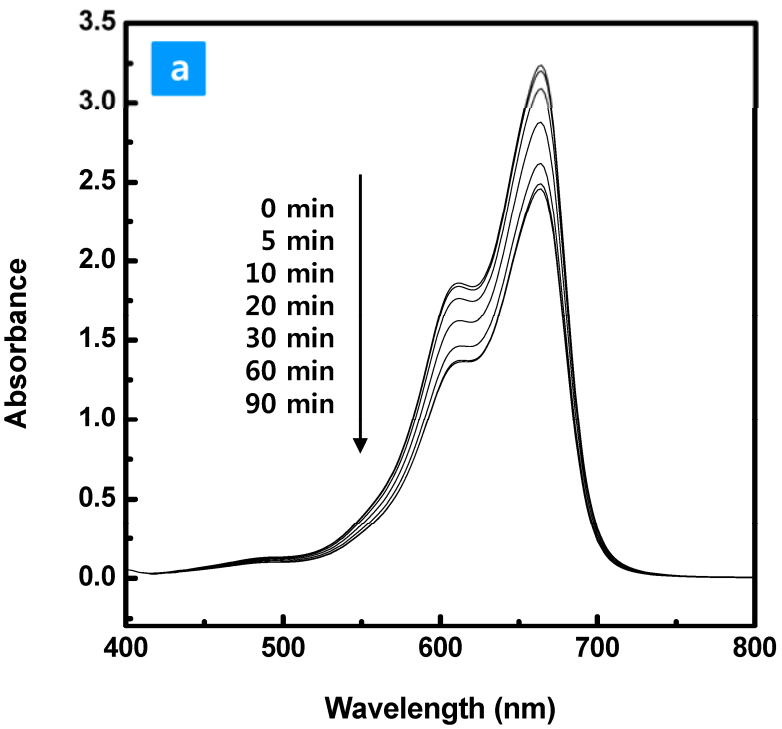
The second-order correlation function  $G_2(\tau)$  can be expressed as a function of the first-order correlation function  $G_1(\tau)$  according to the Siegert relation:  $G_2(\tau) = B(1 + \beta G_1(\tau)^2)$ , where  $B$  is the baseline constant and  $\beta$  is a coherence constant. In the case of a perfect setup, both equal unity. In the case of single-exponential decay,  $G_1(\tau)$  can be expressed in terms of a typical decay rate  $\Gamma$  and time  $t$ ;  $G_1(\tau) = \exp(-\Gamma\tau)$ . The apparent translational diffusion coefficient,  $D$ , is given by equation:  $\Gamma = Dq^2$ , where  $q$  is the magnitude of the scattering vector  $q = 4\pi n \sin(\theta/2)/\lambda$ , where  $n$  is the refractive index of the solvent,  $\theta$  is the scattering angle, and  $\lambda$  is the wavelength of the incident light. For spherical particles, the translational diffusion coefficient can be related to the hydrodynamic radius,  $R$ , according to the Stokes-Einstein equation:  $D = k_B T / 6\pi\eta R$ , where  $D$  is the diffusion coefficient of the Brownian motion of spherical particles,  $k_B$  is the Boltzmann constant,  $T$  is the absolute temperature, and  $\eta$  is the viscosity of the solvent. The hydrodynamic radius distribution of

particles,  $G(R)$  was estimated using the COTIN algorithm, which is conventionally used to determine the inverse Laplace transform of the measured amplitude autocorrelation function.<sup>1, 2</sup>

- (1) R. Finsy, *Adv. Colloid Interfac.* 1994, **52**, 79.
- (2) I. K. Voets, A. De Keizer, M. A. Cohen Stuart and P. De Waard, *Macromolecules* 2006, **39**, 5952.



**Fig. S8** UV-visible spectra of the MH and CQD/MH.



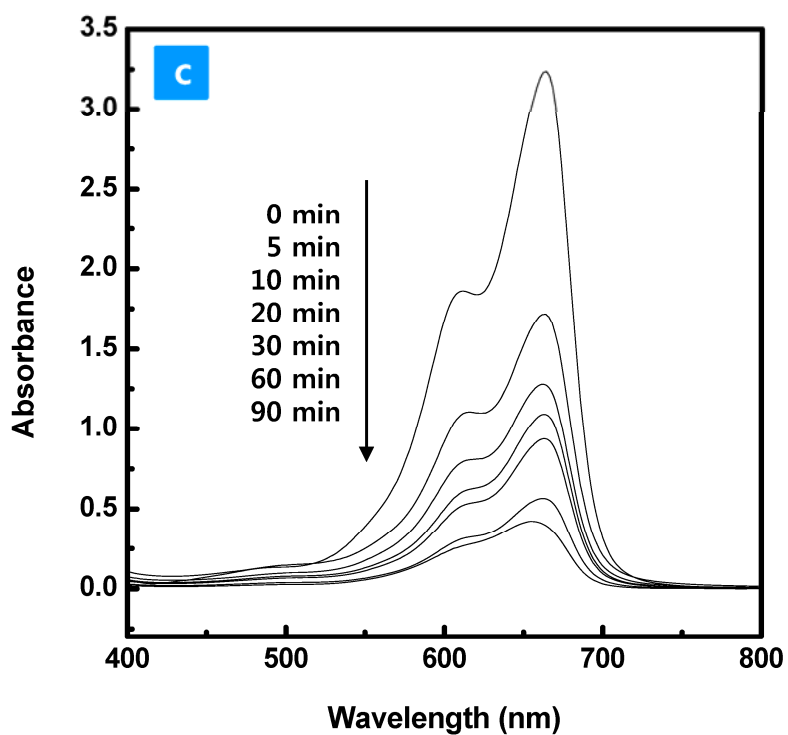


**Fig. S9** Absorption spectra of MB solution taken at different photocatalytic degradation times using (a) MH, (b) MH+H<sub>2</sub>O<sub>2</sub> and (c) CQD/MH.

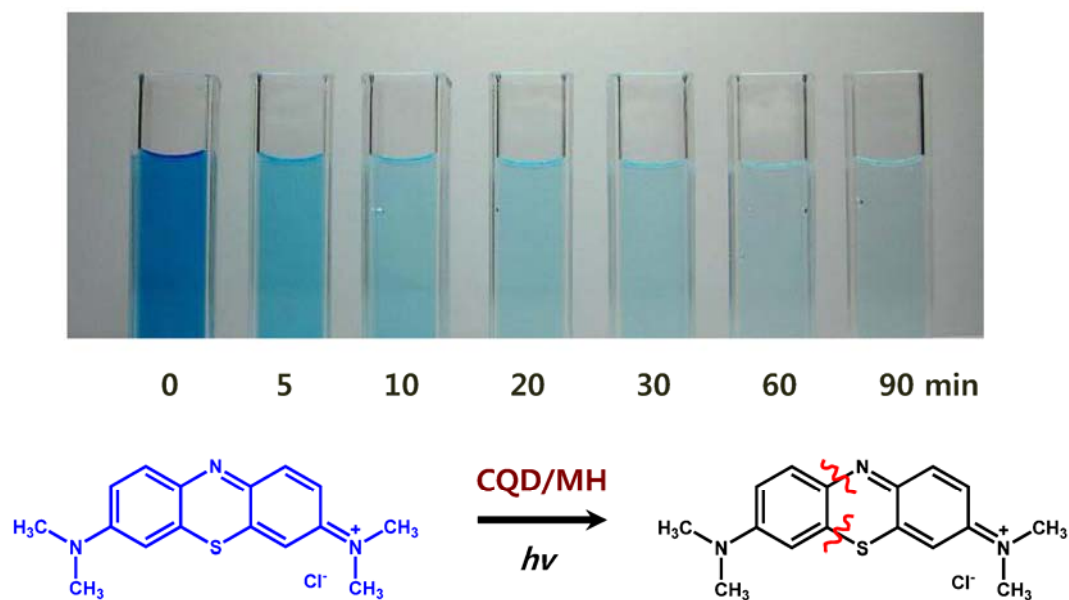


**Fig. S10** Decolorization profiles of MB aqueous solution with visible light irradiation in the presence of the CQD/MH+H<sub>2</sub>O<sub>2</sub>.

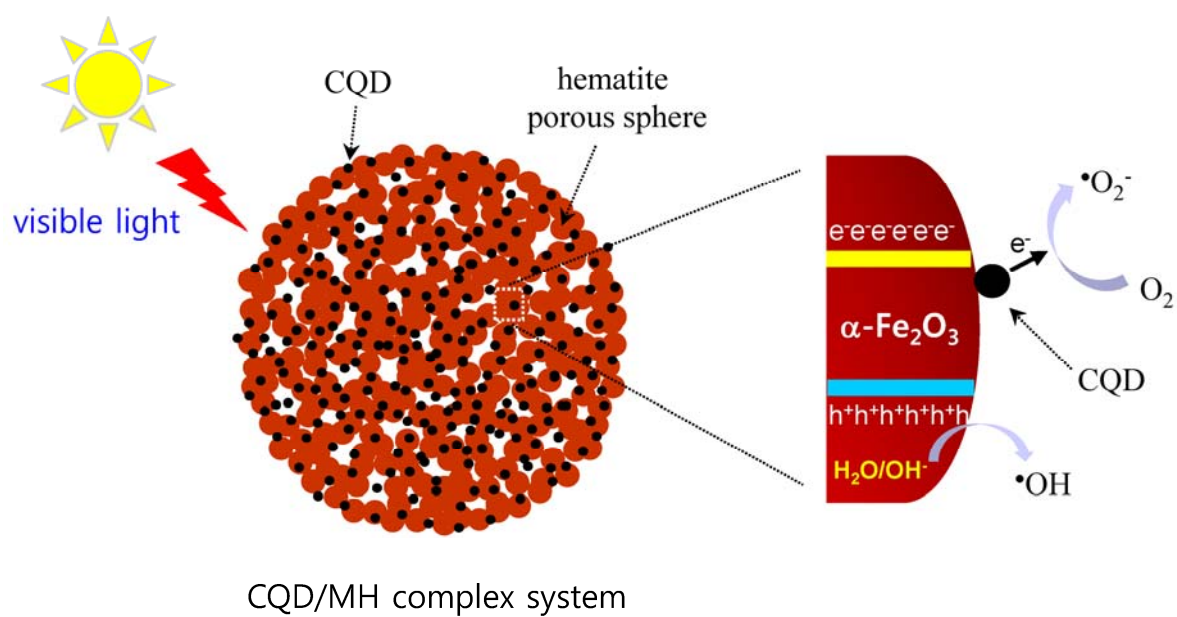


**Fig. S11** Schematic illustration of possible catalytic mechanism for CQD/MH under visible light.